FEBS Letters 377 (1995) 150–154

Crystal structure of an uncleaved α_1-antitrypsin reveals the conformation of its inhibitory reactive loop

Hyun Kyu Song[a], Kee Nyung Lee[b], Ki-Sun Kwon[b], Myeong-Hee Yu[b], Se Won Suh[a,*]

[a]*Department of Chemistry, Center for Molecular Catalysis, Seoul National University, Seoul 151-742, South Korea*
[b]*Protein Engineering Group, Korea Research Institute of Bioscience and Biotechnology, Korea Institute of Science and Technology, Taejon 305-333, South Korea*

Received 1 September 1995; revised version received 7 November 1995

Abstract The crystal structure of a recombinant human α_1-antitrypsin, in the uncleaved and uncomplexed state, has been determined by X-ray crystallographic methods and refined to an *R*-factor of 18.4% for 8.0–3.46 Å data with good stereochemistry. This structure provides the first view at the inhibitory loop and the central β-sheet A of the uncleaved α_1-antitrypsin. The reactive loop takes a distorted helical conformation and no pre-insertion of two residues in the reactive loop into the β-sheet A is observed. The present structure is largely in agreement with the model predicted by Engh, Wright, and Huber [Prot. Eng. 3 (1990) 469–477].

Key words: α_1-Antitrypsin; Inhibitory loop; Molecular replacement; Serpin; X-ray structure

1. Introduction

The serpins (*ser*ine *p*roteinase *in*hibitors) are a ubiquitous family of proteins with diverse functions [1]. They include the proteinase inhibitors of human plasma as well as non-inhibitory plasma proteins [2]. Inhibitory serpins bind to their target enzymes through the reactive site, denoted as P1-P1′ according to the nomenclature of Schecter and Berger [3], which contains the carboxyl and amino-groups, respectively, of the scissile peptide linkage. Serpins share a common tertiary structure with three β-sheets (A–C) and nine α-helices (A–I) [2]. However, the conformations of the reactive loop show striking variations. And known serpin structures have been grouped into four discrete classes: uncleaved non-inhibitory, cleaved at the P1-P1′ junction, active, and latent [4].

Human α_1-antitrypsin (abbreviated here as α_1AT and also known as α_1-proteinase inhibitor), a member of the serpin family, is a glycoprotein of 394 residues. Its genetic deficiency is associated with the lung and liver diseases: for example, the Z variant (Glu342→Lys) leads to emphesyma [5]. A recent study revealed that the Z variant is defective because it folds slowly into the native confomation [6]. The first X-ray structure of inhibitory serpin, that of cleaved α_1AT, showed an unexpected separation of its reactive center peptide bond (Met358–Ser359) by about 70 Å with incorporation of the reactive loop into β-sheet structures [7]. The structure of the intact α_1AT has been modeled based on the assumption that the central strand s4A of the β-sheet A of the cleaved inhibitor is removed from the sheet in the intact inhibitor [8]. This modeling was supported by the X-ray structure of plakalbumin. Here we report the crystal structure of a recombinant human α_1AT in its uncleaved and uncomplexed state. This provides the first view at the reactive loop and the central β-sheet of the uncleaved α_1AT.

*Corresponding author. Fax: (82) (2) 889 1568.
E-mail: sewonsuh@alliant.snu.ac.kr

Abbreviations: serpins, serine proteinase inhibitors; α_1AT, α_1-antitrypsin; r.m.s., root mean square; 9api*, modified α_1-antitrypsin with the reactive loop (P15-P5′, residues 344–363) removed.

2. Materials and methods

The recombinant human α_1AT was purified as described previously [9]. For the crystallization purpose, the purified inhibitor was concentrated to 10 mg/ml by ultrafiltration and then dialyzed against 50 mM Tris-HCl buffer (pH 7.90). Crystallization was achieved by the hanging drop vapor diffusion method at room temperature (22–23°C). Hanging drops were prepared by mixing equal volumes of the protein and the reservoir solutions. Single crystals were grown when the reservoir solution contained 28.5% (w/v) polyethylene glycol 4000, 100 mM Tris-HCl (pH 8.50), and 200 mM lithium sulfate. X-ray data were collected on a FAST TV-area detector (Enraf-Nonius), using the MADNES software [10]. Graphite-monochromatized CuKα X-rays from a rotating anode generator (Rigaku RU-200), running at 40 kV and 70 mA, were used with a 0.3 mm focus cup and a 0.6 mm collimator. The reflection intensities were obtained by the profile fitting procedure of Kabsch [11] and the data were scaled by the Fourier scaling program [12]. The crystal belongs to the monoclinic space group C2 with unit cell dimensions of a = 114.87 Å, b = 39.98 Å, c = 92.42 Å, and β = 102.82 °. There is one α_1AT molecule in the asymmetric unit (V_M = 2.34 Å^3/Da; solvent content = 48%). The completeness of the data set is 81.2% between 35.0 and 3.46 Å, with the data between 3.60 and 3.46 Å being 63.0% complete.

The structure of α_1AT was determined by molecular replacement methods [13,14] using the program package X-PLOR [15] and AMoRe (an Automated package for Molecular Replacement) [16]. Four models were investigated for the molecular replacement: cleaved α_1AT (pdb ID code: 9api, *R*-factor = 20.9% at 3.0 Å resolution) [7], modified α_1AT with the reactive loop (P15-P5′, residues 344–363) removed (denoted as 9api*), cleaved α_1-antichymotrypsin (pdb ID code: 2ach, *R*-factor = 18.7% at 2.7 Å resolution) [17], and ovalbumin (pdb ID code: 1ova, *R*-factor = 16.9% at 1.95 Å resolution) [18]. For molecular replacement calculations, only the non-hydrogen protein atoms in the model were included. A 2σ cutoff based on F was applied to the data throughout the molecular replacement and refinement calculations, unless otherwise noted. The probe structure factors were calculated by placing the starting model in an orthogonal cell with dimensions 100 Å × 100 Å × 100 Å. A consistent solution was obtained with the four starting models and for different resolution ranges. The results of the molecular replacement calculations using AMoRe are summarized in Table 1.

The 9api* model, with the inhibitory loop (P15-P5′, residues 344–363) removed from the cleaved α_1AT, gave the highest correlation coefficient among the four models (Table 1). After orienting and positioning the 9api* model according to the molecular replacement solution, the model was subject to refinement by the program package X-PLOR [15]. Initially a rigid-body refinement was carried out to further improve the values of the positional and orientational parameters. The resolution range of the diffraction data was increased stepwise

SSDI 0014-5793(95)01331-8

Table 1
A summary of AMoRe results[a]

Model[b] (pdb 1D)	Peak rank	Rotation (°)			Translation		R-factor (%)	Correlation coefficient
		α	β	γ	X	Z		
9api	1	295.03	63.97	53.94	0.319	0.251	47.6	0.436
	2	214.96	34.47	68.63	0.445	0.021	53.8	0.292
9api*	1	296.04	61.33	53.22	0.324	0.252	47.2	0.458
	2	26.39	42.23	160.91	0.087	0.381	52.8	0.255
2ach	1	282.98	80.48	236.95	0.318	0.248	43.8	0.424
	2	207.14	42.08	257.55	0.230	0.424	47.3	0.352
1ova	1	296.45	67.50	53.26	0.322	0.244	48.5	0.419
	2	175.54	39.93	256.25	0.306	0.384	52.2	0.267

[a]15.0–4.5 Å data were used.
[b]9api: cleaved α_1-antitrypsin, 9api*: modified α_1-antitrypsin with the reactive loop (P15-P5′, residues 344–363) removed, 2ach: cleaved α_1-antichymotrypsin, 1ova: uncleaved ovalbumin. The number of strands in the central β-sheet A in each model is six for 9api and 2ach and five for 9api* and 1ova.

from 8.0–5.0 to 8.0–3.5 Å. The atomic *B*-factors in the initial model were then changed to 20.0 Å^2 and this value was kept during the next rounds of refinement. The refinement of positional parameters by conventional conjugate gradient minimization reduced the *R*-factor from 41.4 to 27.8% (Table 2). The electron density maps calculated with amplitude coefficients $2F_o-F_c$ and F_o-F_c were used as guides for manual rebuilding of the model using the computer program CHAIN [19]. At this stage the inhibitory reactive loop could be built into the electron density. Finally the model was subject to another round of positional refinement, followed by simulated annealing refinement [20]. The course of crystallographic refinement is summarized in Table 2. Structural comparisons were made using the program LSQKAB in CCP4 program package [21].

3. Results and discussion

The refined model contains 2,965 non-hydrogen protein atoms accounting for 375 amino acid residues of uncleaved α_1AT and no solvent atoms (Fig. 1). The missing residues are the N-terminal 19 residues, which are also missing in the starting model. Final crystallographic *R*-factor is 18.4% for 4,079 unique reflections in the 8.0–3.46 Å resolution range with $F > 2\sigma_F$. The r.m.s. deviations from ideal stereochemistry are 0.015 Å for bond lengths, 2.44° for bond angles, 26.4° for dihedral angles, and 1.9° for improper angles. When the refined model is compared with the starting model (9api*), the r.m.s. deviation for 355 Cα atom pairs (residues 20–343 and 364–394) is 1.8 Å. This indicates that a model bias that is inherent in the molecular replacement solution has been sufficiently reduced during the refinement. As anticipated, the central β-sheet A shows the largest deviation resulting from the closure of the gap between the strands s3A and s5A in the starting model (Fig. 1).

The most pronounced structural difference between the uncleaved and cleaved α_1AT is in the conformation of the reactive loop. The reactive loop of the uncleaved α_1AT, absent in the starting model, is clearly defined by the electron density. As an example, an omit map for a part of the inhibitory loop is shown in Fig. 2. A nearly continuous electron density is observed from Glu354 (P5′ residue) to Glu363 (P5 residue). The reactive loop adopts a distorted helical conformation in the uncleaved α_1AT

Table 2
The course of crystallographic refinement

Stage	Resolution range (Å)	*R*-factor[f] (%)	R.m.s. deviation		Comments
			Bond length (Å)	Bond angle (°)	
1	15.0–4.5	47.2	0.016	2.07	AMoRe solution (9api*[a])
2	8.0–3.5	48.0			Rigid-body refinement (1 rigid group)
3	8.0–3.5	44.0			Rigid-body refinement (23 rigid groups)
4	8.0–3.5	41.4			Rigid-body refinement (36 rigid groups)
5	8.0–3.5	30.0	0.017	2.37	Positional refinement
6	8.0–3.5	27.8	0.016	2.25	Positional refinement
7					Manual model rebuilding
8	8.0–3.5	24.8	0.015	2.42	Positional refinement
9	8.0–3.5	22.7	0.015	2.38	Positional refinement
10					Manual model rebuilding
11	8.0–3.46	20.0	0.016	2.50	Positional refinement
12	8.0–3.46	20.7	0.015	2.35	Prepstage refinement
13	8.0–3.46	18.4	0.015	2.44	Simulated annealing refinement

[f]Reflections with $F_o > 2\sigma_F$.
[a](9api*) Starting model: cleaved α_1-antitrypsin with the reactive loop (P15-P5′, residues 344–363) removed.
[b]At this stage atomic *B*-factors in the starting model were changed to 20.0 Å^2 and this value was kept for the next rounds of refinement (stages 5–13).
[c]The reactive loop (P15-P5′, residues 344–363) was built using $2F_o-F_c$ and F_o-F_c electron density maps.
[d]The problematic regions in the model were rebuilt using $2F_o-F_c$ and F_o-F_c electron density maps.

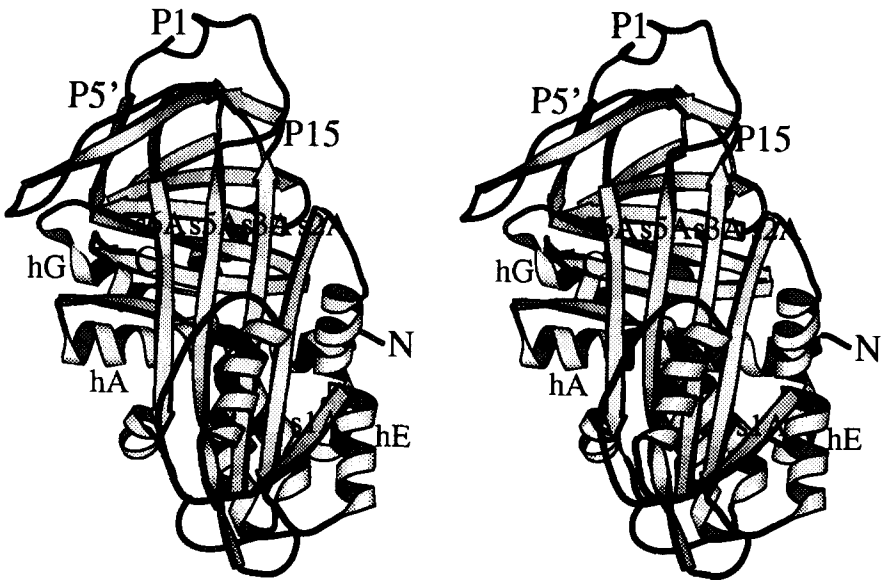

Fig. 1. Stereo ribbon diagram of uncleaved α_1AT drawn with the program MOLSCRIPT [22]. The α-helices are represented by helical ribbons and β-sheets by arrows. The reactive loop residues P15-P5′ (Gly344–Glu363) are at the top.

(Fig. 1, top). The observed conformation of the reactive loop is largely in agreement with the model predicted by Engh, Wright, and Huber [8]. A similar conformation of the reactive loop was also found in a recombinant α_1-antichymotrypsin [23]. In comparison, the reactive loop of ovalbumin, an intact non-inhibitory serpin, takes a helical conformation. Further variations of the reactive loop have been observed in the crystal structure of antithrombin, for which one active molecule has its partially inserted reactive loop in the central β-sheet A (termed 'pre-insertion') and the other inactive molecule has a totally incorporated loop as in latent plasminogen activator inhibitor-1 [24,25].

A comparison of the central β-sheet A (lying vertically in Figs. 1 and 3) in the uncleaved α_1AT with those in other structures of serpins reveals interesting differences as well as similarities. In the uncleaved α_1AT, the strand s4A of β-sheet A in the cleaved α_1AT is removed from the sheet (Fig. 3a). A superposition of 54 Cα atoms in the central β-sheet A [s2A (residues 109–121), s3A (residues 181–194), s5A (residues 326–342), and s6A (residues 290–299)] of the present model of uncleaved α_1AT and the corresponding atoms in the cleaved α_1AT model (9api) gives an r.m.s. difference of 2.4 Å (Fig. 3a). In contrast, a superposition of the above 54 Cα pairs in the uncleaved α_1AT and ovalbumin (1ova) gives a much smaller r.m.s. difference of

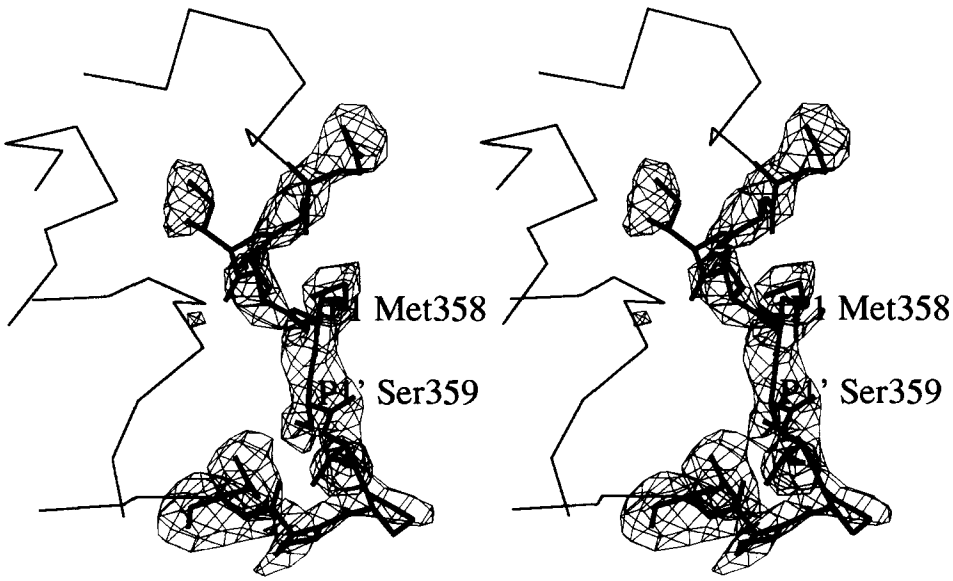

Fig. 2. An (F_o–F_c) omit map for a part of the reactive loop, contoured at 2.5 σ. The map was generated using data in the range 8.0–3.46 Å and phases calculated from the current model with ten residues P5-P5′ (Glu354–Glu363) omitted. The refined model of the omitted region is drawn in thick lines and P1 Met358 and P1′ Ser359 are indicated. Other parts of the model are drawn by Cα tracings in thin lines.

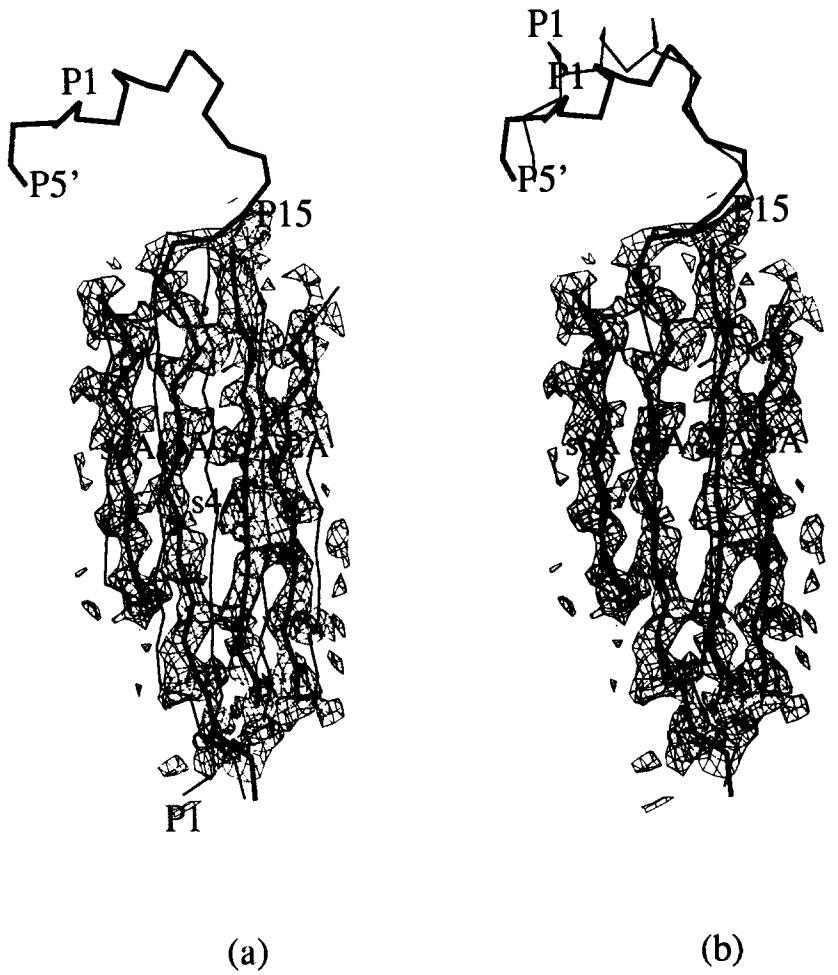

Fig. 3. A stereo view of the final $(2F_o-F_c)$ electron density map and the central β-sheet A of uncleaved α_1AT (in thick lines). The reactive loop of uncleaved α_1AT is also shown at the top of the figure. Thin lines in (a) and (b) represent the superposed models of cleaved α_1AT and ovalbumin, respectively. The strands of the central β-sheet A are labelled as s2A, s3A, s4A, s5A, and s6A, respectively. The P15, P1, and P5′ sites of the reactive loops are also indicated.

1.5 Å (Fig. 3b). Thus it is found that the central β-sheet A of the uncleaved α_1AT is largely similar to that of ovalbumin. This is easily understood because the N-terminal part of the reactive loop in the cleaved α_1AT structure is fully inserted into the central β-sheet A to form the strand s4A, whereas the reactive loop in ovalbumin forms a helix at the top of the molecule, leaving β-sheet A with one less strand (Fig. 3b). The reactive loop of the uncleaved α_1AT, adopting a distorted helical conformation, lies a little closer to the main body than that of ovalbumin (Fig. 3b). This may be partly due to the crystal packing. The reactive loop of our uncleaved α_1AT makes a 'head-to-head' contact with a symmetry-related molecule in the crystal.

Another example of serpin for which both the intact and cleaved structures are known is antithrombin. A superposition of 61 Cα atom pairs in the central β-sheet A, excluding the very different reactive loop, gives an r.m.s. difference of 1.7 Å [26]. This intermediate difference is a consequence of the wider opening between the strands s3A and s5A in the β-sheet A, which allows a partial insertion of two s4A residues. In contrast, no pre-insertion of the two N-terminal residues of the reactive loop is observed for the uncleaved α_1AT in this study as well as for the uncleaved α_1-antichymotrypsin [23].

In summary, the present structure, albeit at a somewhat low resolution, shows for the first time that the reactive loop of uncleaved α_1AT in the uncomplexed state adopts a distorted helical conformation and no pre-insertion of two s4A residues into the central β-sheet A takes place.

Acknowledgements: We thank the Korea Ministry of Education, Basic Sciences Research Institute Program (S.W.S.), Center for Molecular Catalysis (S.W.S.), and the Korea Ministry of Science and Technology (M.-H.Y., Grant G71142) for financial support. We also thank the Inter-University Center for Natural Science Research Facilities for providing the X-ray equipments. The coordinates will be deposited with the Protein Data Bank.

References

[1] Travis, J. and Salvesen, G. S. (1983) Annu. Rev. Biochem. 52, 655–709.
[2] Stein, P.E. and Carrell R.W. (1995) Nature Struct. Biol. 2, 96–113.
[3] Schecter, I. and Berger, A. (1967) Biochem. Biophys. Res. Commun. 27, 157–162.

[4] Fletterick, R.J. and McGrath, M.E. (1994) Nature Struct. Biol. 1, 201–203.
[5] Crystal, R.G. (1989) Trends Genet. 5, 411–417.
[6] Yu, M.-H., Lee, K.N. and Kim, J. (1995) Nature Struct. Biol. 2, 363–367.
[7] Loebermann, H., Tokuoka,R., Deisenhofer, J. and Huber, R. (1984) J. Mol. Biol. 221, 615–621.
[8] Engh, R.A., Wright, H.T. and Huber, R. (1990) Protein Eng. 3, 469–477.
[9] Kwon, K.-S., Lee, S. and Yu, M.-H. (1995) Biochim. Biophys. Acta 1247, 179–184.
[10] Messerschmidt, A. and Pflugrath, J.W. (1987) J. Appl. Crystallogr. 20, 306–315.
[11] Kabsch, W. (1988) J. Appl. Crystallogr. 21, 916–924.
[12] Weissman, L. (1982) in: Computational Crystallography (Sayre, D., Ed.) pp. 56–63, Oxford Univ. Press (Claredon), Oxford.
[13] Crowther, R.A. (1972) in: The Molecular Replacement Method, a Collection of Papers on the Use of Non-Crystallographic Symmetry (Rossmann, M.G., Ed.) pp. 173–178, Gordon and Breach, New York.
[14] Crowther, R.A. and Blow, D.M. (1967) Acta Crystallogr. 23, 544–548.
[15] Brünger, A.T. (1992) in: X-PLOR Manual, Version 3.1: A System for Crystallography and NMR, Yale University Press, New Haven.
[16] Navaza, J. (1994) Acta Crystallogr. A50, 157–163.
[17] Baumann, U., Huber, R., Bode, W., Lesjak, G.M. and Laurell, C.B. (1991) J. Mol. Biol. 218, 595–606.
[18] Stein, P.E., Leslie, A.G.W., Finch, T.J., Turnell, W.G., McLaughlin, P.J. and Carrell, R.W. (1990) Nature 347, 99–102.
[19] Sack, J.S. (1988) J. Mol. Graphics 6, 244–245.
[20] Brünger, A.T. and Krukowski, A. (1990) Acta Crystallogr. A46, 585–593.
[21] SERC Daresbury Laboratory (1994) Acta Crystallogr. D50, 760–763.
[22] Kraulis, P.J. (1991) J. Appl. Crystallogr. 24, 946–950.
[23] Wei, A., Rubin, H., Cooperman, B.S. and Christianson, D.W. (1994) Nature Struct. Biol. 1, 251–258.
[24] Carrell, R.W., Stein, P.E., Fermi, G. and Wardell, M.R. (1994) Structure 2, 257–270.
[25] Mottonen, J., Strand, A., Symersky, J. Sweet, R.M., Danley, D.E., Geoghegan, K.F., Gerard, R.D. and Goldsmith, E.J. (1992) Nature 355, 270–273.
[26] Schreuder, H.A., Boer, B., Dijkema, R., Mulders, J., Theunissen, H.J.M., Grootenhuis, P.D.J. and Hol, W.G.J. (1994) Nature Struct. Biol. 1, 48–54.